

Multiband Patch Antenna Design Using Nature-Inspired Optimization Method

ACHILLES D. BOURSANIS¹ (Member, IEEE), MARIA S. PAPADOPOULOU¹, JULIANO PIEREZAN²,
VIVIANA C. MARIANI³, LEANDRO S. COELHO^{2,3}, PANAGIOTIS SARIGIANNIDIS⁴, (Member, IEEE),
STAVROS KOULOURIDIS⁵ (Member, IEEE), AND SOTIRIOS K. GOUDOS¹ (Senior Member, IEEE)

¹ELEDIA@AUTH Research Group, School of Physics, Aristotle University of Thessaloniki, 54124 Thessaloniki, Greece

²Department of Electrical Engineering, Federal University of Parana, Curitiba 80060-000, Brazil

³Industrial and Systems Engineering Graduate Program and Mechanical Engineering Graduate Program,
Pontifical Catholic University of Parana, Curitiba 80215-901, Brazil

⁴Department of Electrical and Computer Engineering, University of Western Macedonia, 501 00 Kozani, Greece

⁵Electrical and Computer Engineering Department, University of Patras, 26504 Patras, Greece

CORRESPONDING AUTHOR: A. D. BOURSANIS (e-mail: bach@physics.auth.gr)

This research was supported in part by the European Regional Development Fund of the European Union and Greek
in part by national funds through the Operational Program Competitiveness, Entrepreneurship and Innovation,
under the call RESEARCH—CREATE—INNOVATE under project T1EDK-05274.

ABSTRACT Radio frequency energy harvesting has attracted considerable interest as a technique of enabling self-powered wireless networks. This technique faces several challenges, such as the receiving and the rectifying modules of a rectenna system. Multiband antennas provide several comparative advantages against the goal of maximizing the amount of energy harvesting. In this work, we present a multiband microstrip patch antenna with three slits operating in the LoRaWAN (Long Range Wide Area Network) and the cellular (GSM-1800 and UMTS) communication frequency bands. A feasible solution of the antenna is obtained by the application of a recently introduced nature-inspired optimization technique, namely the Coyote Optimization Algorithm. The proposed antenna operates satisfactorily in the LoRaWAN (Long Range Wide Area Network) and the cellular (GSM-1800 and UMTS) communication frequency bands. Measured results of the proposed antenna exhibit an acceptable performance (multiband frequency operation, maximum gain of 3.94 dBi, broadside operation) and demonstrate features of operation, which make it a strong candidate for various RF energy harvesting applications.

INDEX TERMS Microstrip line, multiband antenna, optimization method, patch antenna, radio frequency energy harvesting.

I. INTRODUCTION

ENERGY Harvesting (EH) is one of the most promising techniques for self-powered systems that require small amounts of energy to operate [1]. As an alternative technique, it is expected to bring several changes in legacy wireless networking [2], such as wireless sensor networks, which are dominated through their deployments in the Internet of Things (IoT) and Cyber-Physical Systems (CPS) [3], [4]. Radio Frequency EH can play a pivotal role in next-generation wireless networks [5] or environmental wireless sensor networks [6], since the primary characteristic

of these networks is ultra-low power consumption. The availability of power transmission on a 24-hour basis and the spatial coverage of transmitted power from ambient sources mostly in urban areas are two of the main comparative characteristics of RF EH against other popular EH techniques (solar, piezoelectric, thermal, etc.) [7], [8]. Therefore, RF EH from ambient and dedicated sources is an attractive choice in wireless power transfer (WPT) with considerable benefits in usability, design, availability, and reliability [8], [9]. A typical RF EH system consists of a rectenna (antenna + rectifier), which is the combination of

an antenna, an impedance matching network, and a rectifying circuit [10].

Microstrip patch antenna is an attractive design approach that offers several advantages in RF energy harvesting systems [11], [12]. These include, among others, the relatively small physical dimensions of the antenna compared to the wavelength of the desired frequency, the medium complexity in the design, the low cost, and the ease of fabrication [4], [13], [14]. The characteristics and the overall performance (by the key performance numbers of reflection coefficient, bandwidth, and gain) are also important features of the antenna design for RF energy harvesting applications [15], [16].

Meta-heuristics are one of the two classes of stochastic algorithms (the other one is heuristics) that are utilized to provide solutions in sophisticated optimization problems [17]. Generally speaking, they usually perform better than the heuristic algorithms, because they apply certain trade-off between randomization and local search mechanisms [18]. Meta-heuristic algorithms can be divided into two main categories: nature-inspired [19] and human-based algorithms [20].

Nature-inspired algorithms can be further split into evolutionary [21], swarm-intelligence [22], [23], and physics-based algorithms [24]. Among the most widely-known meta-heuristic algorithms are included the Genetic Algorithm (GA) [25], the Particle Swarm Optimization (PSO) [26], [27], the Biogeography-Based Optimization (BBO) [28], the Simulated Annealing (SA) [29], the Teaching Learning Based Optimization [30], and the Grey Wolf Optimizer [22]. Coyote Optimization (CO) is a newly introduced meta-heuristic algorithm that describes the social behavior within the packs of *Canis latrans*, or the so-called coyote or brush wolf [31]. It is a population-based and nature-inspired algorithm.

In this work, we present a feasible solution of a multiband patch antenna with three slits that operates within the European LoRaWAN (Long Range Wide Area Network), as well as the GSM-1800 and UMTS cellular communication frequency bands. This solution is obtained by combining a recently introduced nature-inspired meta-heuristic algorithm, namely the Coyote Optimization Algorithm, and a powerful high-frequency electromagnetic solver. To the best of the authors' knowledge, this is the first time that the CO algorithm is utilized to handle an electromagnetic problem. The proposed antenna is fabricated and experimentally evaluated. It demonstrates features of operation, which make it a promising candidate for RF energy harvesting applications.

The rest of this work is structured as follows. Section II outlines the related work in this research topic. Section III briefly describes the Coyote Optimization Algorithm and its mechanisms to provide solutions to an optimization problem, as well as evaluates its performance against other popular nature-inspired algorithms. Section IV analyses the optimization method applied to obtain a feasible solution for the geometry of the proposed antenna. Section V presents

in detail the obtained results of the fabricated antenna and performs a comparison of its characteristics against related published work. Finally, Section VI concludes our findings of this work and gives some future directions.

II. RELATED WORK

A multiband receiving module (antenna) in a rectenna system provides a comparative advantage against an antenna operating in a single band, i.e., the capability to harvest higher values of electromagnetic radiation [15]. However, the choice of a multiband antenna in an RF harvesting system draws and some disadvantages, such as the increased complexity of the system, but mostly, the difficulty of the matching network to operate sufficiently at different frequency bands. Multiband antennas for RF energy harvesting applications have been extensively studied in the literature. Several types of antennas with low, medium, and high complexity have been tested and evaluated as RF energy harvesting modules in rectenna systems.

These include monopole [32], [33], [34], [35], dipole [36], [37], [38], [39], bow-tie [40], log-periodic [41], and yagi-UDA [42] antennas, as RF EH receiving modules with low complexity; multi-slot [43], [44], inverted-F [45], spiral [46], and patch [47], [48], [49] antennas with medium complexity; fractal [50], [51] and reconfigurable [52] antennas, as RF EH modules with high complexity. Moreover, sophisticated complex systems [53], [54], [55], [56], [57] operating as RF energy harvesters in multi-frequency bands have also been reported in the literature. Finally, the type of antenna arrays [58], [59], [60] have also been successfully evaluated as multiband RF EH systems.

III. CO ALGORITHM

A. ALGORITHM DESCRIPTION

The population-based and nature-inspired algorithm denoted Coyote Optimization Algorithm (COA) was proposed by [31] and the social relations inside the packs of the *Canis latrans* has served as inspiration. The first step of the algorithm is the definition of the initial population of coyotes, which implies on $N_p \in \mathbb{N}^*$ packs with $N_c \in \mathbb{N}^*$ coyotes each. The initial packs' division is randomly selected. The decision variables are referred as "social condition", and the values of the c^{th} coyote of the p^{th} pack in the j^{th} dimension are defined as:

$$soc_{c,j}^{p,t} = lb_j + r_j \cdot (ub_j - lb_j) \quad (1)$$

wherein lb_j and ub_j correspond to the boundaries of the j^{th} decision variable, and $r_j \in [0, 1]$ is a uniformly distributed random number.

The second step is the calculation of the objective function values for each set of decision variables, which means:

$$fit_c^{p,t} = f(soc_c^{p,t}) \quad (2)$$

The COA considers the coyote's transition between packs, which depends on N_c and occurs with probability P_e , such

Algorithm 1 Maintenance and Rejection Within a Pack of Coyotes

```

1: Compute  $\omega$  and  $\varphi$ 
2: if  $\varphi = 1$  then
3:   The young coyote is maintained and the only coyote
   in  $\omega$  group is rejected.
4: else
5:   if  $\varphi > 1$  then
6:     The young coyote is maintained and the oldest
     coyote in  $\omega$  is rejected.
7:   else
8:     The young coyote is maintained.
9:   end if
10: end if

```

that:

$$P_e = 0.005 \cdot N_c^2 \quad (3)$$

Furthermore, the CO algorithm takes into account the alpha coyote, i.e., the coyote with the best objective function cost value in the p^{th} pack of the t^{th} timestamp. It is defined as:

$$alpha^{p,t} = \{soc_c^{p,t} | arg_{c=\{1,2,\dots,N_c\}} minf(soc_c^{p,t})\} \quad (4)$$

The COA also regards the cultural trend, which is estimated inside each pack. The calculation occurs as follows:

$$ct_j^{p,t} = \begin{cases} O_{\frac{(N_c+1)}{2}j}^{p,t}, & N_c \text{ is odd} \\ \frac{O_{\frac{N_c}{2}j}^{p,t} + O_{\frac{(N_c+1)}{2}j}^{p,t}}{2}, & \text{otherwise} \end{cases} \quad (5)$$

where $O^{p,t}$ represents the ranked social conditions of all coyotes of the p^{th} pack in the t^{th} instant of time for every j in the range $[1, D]$, D is the search space dimension.

The algorithm syncs the birth and the death of the coyotes, which depends on the values of the objective function and the coyotes' ages (it is computed in years and defined as $age_c^{p,t} \in \mathbb{N}$). This mechanism is described in the Algorithm 1, where ω represents the group of coyotes with the worst score in objective function's values and φ defines the total number of coyotes in this group. The group of ω coyotes is derived by comparing the objective function values of the young coyote (pup) and all the coyotes of the pack.

The pups are generated through the incorporation of the social conditions of two randomly chosen parents plus an environmental factor. The parents are selected regardless of their social conditions. As a result, the pups are defined as:

$$pup_j^{p,t} = \begin{cases} soc_{r_1,j}^{p,t}, & rnd_j < P_g \text{ or } j = j_1 \\ soc_{r_2,j}^{p,t}, & rnd_j \geq P_d + P_g \text{ or } j = j_2 \\ R_j, & \text{otherwise} \end{cases} \quad (6)$$

wherein r_1 and r_2 are the two designated coyotes from the p^{th} pack, j_1 and j_2 are two random dimensions of the optimization problem, P_s is the scatter probability, P_a is the association probability, R_j is a random number limited to

the boundaries of the decision variables of the j^{th} dimension, and rnd_j is a uniformly generated random number $\in [0, 1]$.

The scatter and association probabilities (P_s and P_a , respectively) conduct the coyotes' diversity. These values are calculated as follows:

$$P_s = 1/D \quad \text{and} \quad (7)$$

$$P_a = (1 - P_d)/2 \quad (8)$$

where P_a balances the influence impact equally for both parents.

The coyotes are under the whole pack influence (δ_t) and the alpha influence (δ_a), which are written respectively as:

$$\delta_t = ct^{p,t} - soc_{cr_1}^{p,t} \quad \text{and} \quad (9)$$

$$\delta_a = alpha^{p,t} - soc_{cr_2}^{p,t} \quad (10)$$

where cr_1 denotes the cultural difference from a random coyote and cr_2 denotes the cultural difference between a random coyote of the pack and the alpha coyote.

Considering that r_t and r_a are the pack and the alpha influence weights respectively, which are uniformly distributed random numbers $\in [0, 1]$, the coyote's new social condition is updated using the following equation:

$$new_soc_c^{p,t} = soc_c^{p,t} + r_t \cdot \delta_t + r_a \cdot \delta_a \quad (11)$$

while new social condition is expressed as:

$$new_fit_c^{p,t} = f(new_soc_c^{p,t}) \quad (12)$$

The best social condition is reserved, which means:

$$soc_c^{p,t+1} = \begin{cases} new_soc_c^{p,t}, & new_fit_c^{p,t} < fit_c^{p,t} \\ soc_c^{p,t}, & \text{otherwise} \end{cases} \quad (13)$$

and the final solution of the algorithm is the best solution among all packs. As an initial guess, N_c can be set in the range $[5, 10]^1$ and N_p can be subsequently adjusted to define the total population size of the algorithm. Fig. 1 illustrates the algorithmic sequence of the Coyote Optimization Algorithm mechanisms.

The time complexity of the CO algorithm is similar to that of other evolutionary algorithms, i.e., at each iteration is $\mathcal{O}(N_p N_c D + N_p N_c f)$, where f is the time complexity of the objective function and D is the search space dimension.

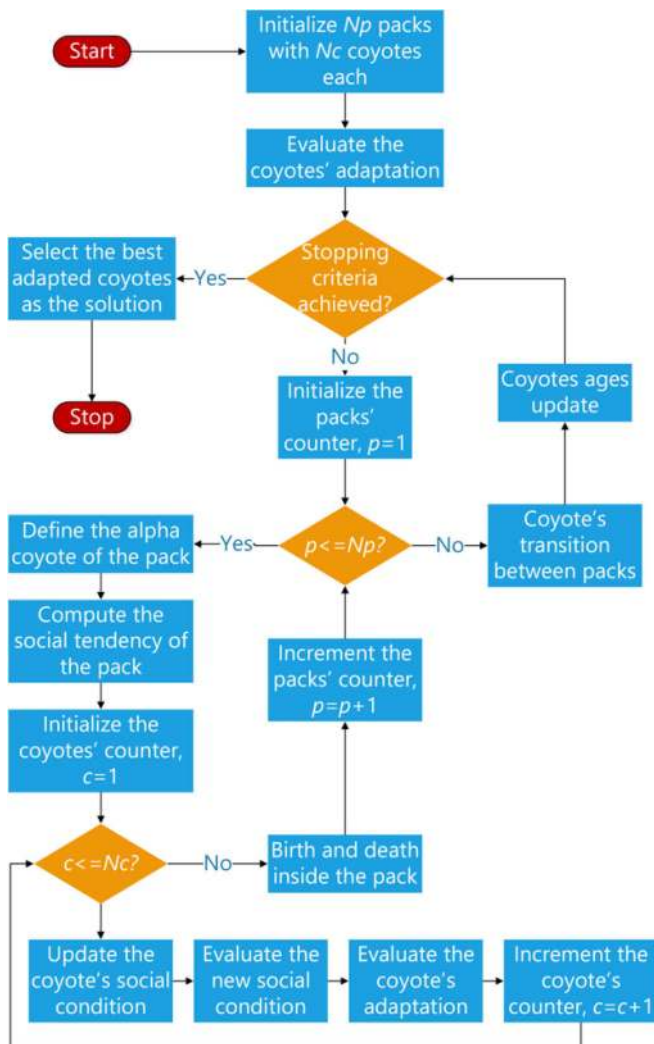
B. PERFORMANCE EVALUATION

The CO algorithm is evaluated in terms of its performance against 5 widely-known meta-heuristic algorithms, namely the Particle Swarm Optimization (PSO) [26], the Firefly Algorithm (FA) [61], the Bees Algorithm (BA) [62], the Harmony Search (HS) [63], and the Ant Colony Optimization (ACO) [64]. The algorithms' performance is assessed by utilizing 10 common benchmark functions (f_1 : Ackley, f_2 : Griewank, f_3 : Rastrigin, f_4 : Schaffer, f_5 : Shubert, f_6 : Booth, f_7 : Rozenbrock, f_8 : Michalewicz, f_9 : Goldstein-Price, and

1. In the original proposal, the COA has scored good performance with N_p equals to 5.

TABLE 1. Performance score of the meta-heuristic algorithms for each of the selected benchmark functions (the best (smallest) values are indicated in bold).

Benchmark Function	COA	PSO	FA	BA	HS	ACO
f_1	5.87E-02	3.06E-14	7.78E-10	9.66E+00	4.44E-03	5.63E+00
f_2	1.48E-03	3.61E-03	2.05E-03	1.05E+00	3.78E-03	8.86E-01
f_3	9.16E+00	5.63E+01	3.46E+01	4.05E+02	2.82E+00	3.30E+02
f_4	0.00E+00	0.00E+00	0.00E+00	1.34E-07	4.12E-06	0.00E+00
f_5	-1.87E+02	-1.87E+02	-1.87E+02	-1.87E+02	-1.87E+02	-1.86E+02
f_6	0.00E+00	0.00E+00	3.97E-24	0.00E+00	1.42E-09	0.00E+00
f_7	9.80E+01	1.99E+01	9.14E+00	2.02E+05	8.81E+01	3.10E+05
f_8	-2.87E+01	-1.93E+01	-2.50E+01	-2.28E+01	-2.84E+01	-6.24E+00
f_9	3.00E+00	3.00E+00	3.00E+00	3.00E+00	6.60E+00	3.00E+00
f_{10}	-3.86E+00	-3.86E+00	-3.86E+00	-3.86E+00	-3.86E+00	-3.86E+00

**FIGURE 1.** Flowchart of the Coyote Optimization Algorithm's main mechanisms.

f_{10} : Hartmann 3-D) with various characteristics (many local minima, plate-shaped, valley-shaped, steep drops, etc.) [65]. For the assessment of the COA's performance against the other meta-heuristic algorithms, the following parameters are applied:

TABLE 2. Friedman's non-parametric ranking test (the best (smallest) values are indicated in bold).

Algorithm	Mean Ranking
COA	2.65
PSO	2.95
FA	2.8
BA	4.4
HS	3.75
ACO	4.45

- Number of decision variables: 30
- Boundaries of decision variables: $[-10 \ 10]$
- Population number: 100
- Maximum number of iterations: 1000
- Number of independent trials: 30

Table 1 lists the performance score (mean value of the computed cost function over the set independent trials) for each of the previously mentioned algorithms. From the listed results, we can conclude that the CO algorithm outperforms in 7 of the 10 benchmark functions, PSO outperforms in 6 of the 10 functions, and FA outperforms in 5 of the 10 functions. It is also noteworthy that, for some benchmark functions (f_4 , f_5 , f_6 , f_9 , f_{10}), more than one algorithm achieves the same performance score. To further assess the computed results of the meta-heuristic algorithms, the Friedman test is applied. This non-parametric test utilizes the mean values of the computed cost function for every optimization method over the set of the independent trials to rank the given algorithms based on their performance.

Table 2 lists the computed results of the Friedman non-parametric test. From the given results, we can conclude that the CO algorithm achieves the best mean ranking, FA is second in the ranking list, and PSO obtains the third-best score. We should also point out that the differences in the mean ranking between the first three algorithms in the list, i.e., COA, FA, and PSO, are relatively small. However, from the presented results, the CO algorithm exhibits a small

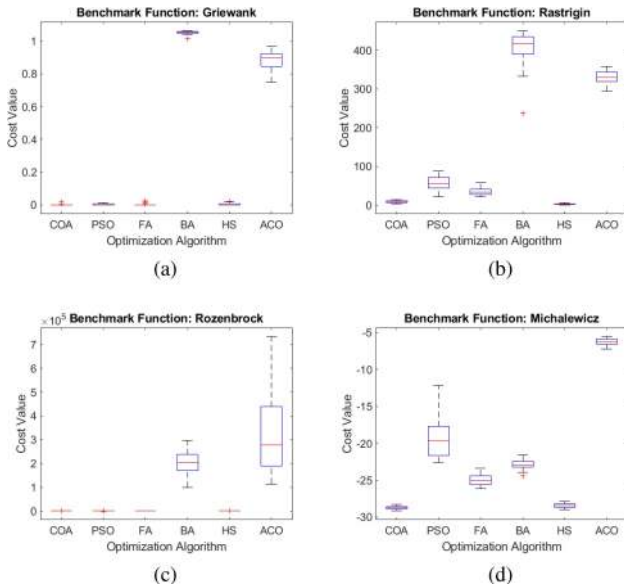


FIGURE 2. Boxplot distribution of the computed cost function for the meta-heuristic algorithms over representative benchmark functions (a) f_2 : Griewank, (b) f_3 : Rastrigin, (c) f_7 : Rozenbrock, and (d) f_8 : Michalewicz.

lead in terms of its performance against the FA and PSO algorithms.

Finally, Fig. 2 illustrates the boxplot distribution of the computed cost function for each of the aforementioned meta-heuristic algorithms. Four representative examples of equally benchmark functions are selected to demonstrate the COA performance against the other optimization algorithms. From the presented graphs we can conclude that the 50-percentile values (median) of the cost function of the COA for each of the selected benchmark functions presents competitive performance when compared to the boxplot distribution of the other algorithms' cost functions. It is also noteworthy that the 25-percentile and the 75-percentile of the cost function value for the CO algorithm show indiscernible variation, thus exhibiting the algorithm's stability and durability.

IV. ANTENNA OPTIMIZATION PROCEDURE

The optimization process to obtain a feasible solution of a multiband patch antenna that can be suitable for RF EH applications is taking place by the interaction between the Coyote Optimization algorithm and the utilization of a powerful commercial high-frequency electromagnetic solver (HFSS, © 2020 ANSYS, Inc.).

Fig. 3 illustrates the proposed patch antenna geometry. The proposed antenna consists of a rectangle patch with three different slits of various sizes. From Fig. 3(b), we can easily derive that the social condition vector (vector of the decision variables) consists of 14 elements, thus 14 design parameters are required to define the proposed antenna geometry. The antenna is fed by the use of a microstrip line. It is designed on a single FR-4 substrate layer (thickness = 1.6 mm, relative permittivity $\epsilon_r = 4.4$, $\tan\delta = 0.02$). A ground plane is placed beneath the FR-4 substrate. Finally, boundary conditions of

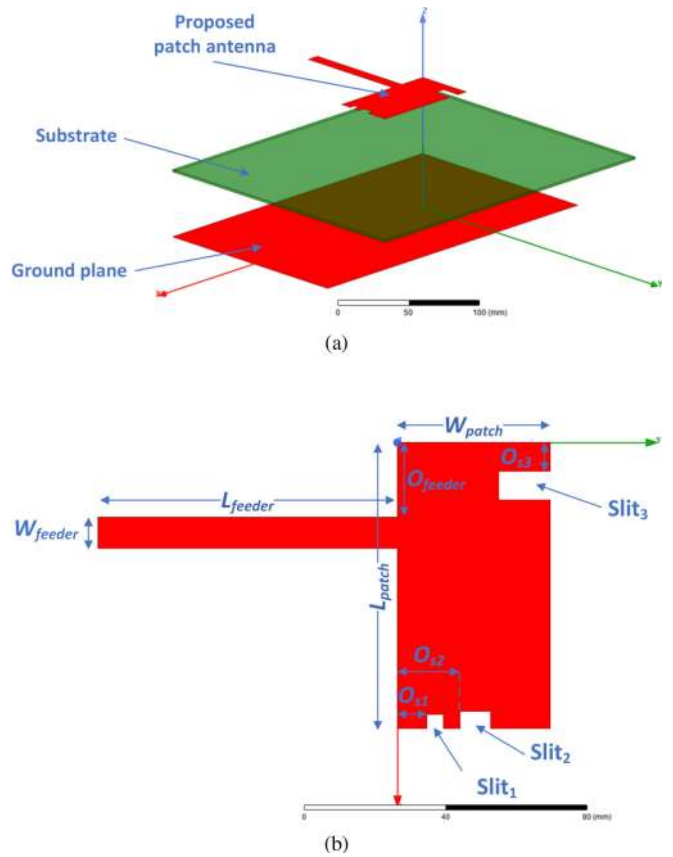


FIGURE 3. Geometry of the proposed microstrip patch antenna: (a) expanded perspective view (red color: ground plane and the proposed patch antenna, green color: FR-4 dielectric substrate), (b) plane view (the decision variables of the optimization process are indicated).

finite conductivity (conductivity = $5.80E + 07$ Siemens/m, relative permeability = 1) are applied to the patch antenna, the microstrip line, and the ground plane.

One may observe that the proposed antenna geometry is rather complex and requires the proper setting of 14 different design parameters. Hence, it would be quite difficult or even impossible to assess the effect of each design parameter in order to meet the desired antenna performance using a trial-and-error procedure. Thus, we need to apply an optimization algorithm to solve this type of problem. In this case, we apply the recently introduced Coyote Optimization algorithm.

In this work, the objective of the optimization problem is to minimize the S_{11} magnitude of the proposed antenna at three (at least) different frequencies within the frequency bands of European LoRaWAN (Long Range Wide Area Network) (863 MHz - 870 MHz), the Global System for Mobile Communications GSM-1800 (1710 MHz - 1880 MHz), and the Universal Mobile Telecommunications System (UMTS) (1905.1 MHz - 2155.3 MHz) communication systems. A solution provided by the optimization process can be accepted if the reflection coefficient value is equal or less than a criterion limit. For the optimization of a patch antenna for RF EH applications, the criterion limit is set to -10 dB. Therefore, the objective function of the given

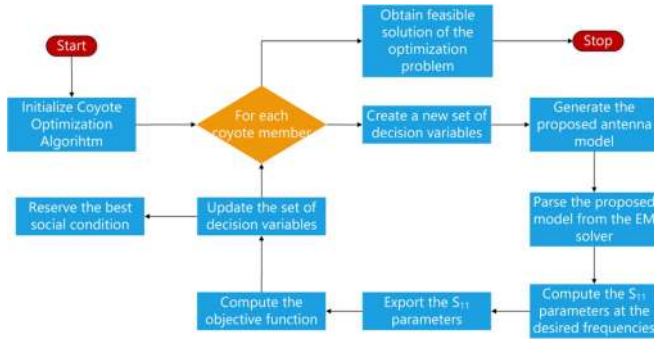


FIGURE 4. Process to obtain a feasible solution for a given optimization problem by applying the CO algorithm.

problem can be expressed as

$$\begin{aligned}
 \text{Minimize } F(\bar{x}) = & \max\left(S_{11}^{868\text{MHz}}(\bar{x}), S_{11}^{1.8\text{GHz}}(\bar{x}), S_{11}^{2.1\text{GHz}}(\bar{x})\right) \\
 & + \Psi \times \max\left(0, S_{11}^{868\text{MHz}}(\bar{x}) - L_{\text{dB}}\right) \\
 & + \Psi \times \max\left(0, S_{11}^{1.8\text{GHz}}(\bar{x}) - L_{\text{dB}}\right) \\
 & + \Psi \times \max\left(0, S_{11}^{2.1\text{GHz}}(\bar{x}) - L_{\text{dB}}\right) \quad (14)
 \end{aligned}$$

where \bar{x} is the vector of the proposed antenna geometry parameters (social condition or decision variables of the optimization process), $S_{11}^{868\text{MHz}}$, $S_{11}^{1.8\text{GHz}}$ and $S_{11}^{2.1\text{GHz}}$ are the S_{11} parameters (reflection coefficient) of the proposed antenna, L_{dB} is the S_{11} criterion limit in dB, and Ψ is a very large factor ($1E+10$) that is assigned to the current solution of the problem when the criterion limit is not satisfied.

Fig. 4 illustrates the general concept of the aforementioned optimization process. Firstly, we define the algorithm's parameters (N_p , N_c , $MaxIt$: maximum number of iterations), as well as the upper (ub_j) and lower (lb_j) boundaries of the optimization process. Secondly, for each coyote member of the population N ($N = N_p \times N_c$), a set of decision variables (social condition) is determined using (1) and an antenna model is created. The proposed model is parsed from the EM solver to compute the reflection coefficients (S_{11} parameters) at the frequencies of interest. These values of reflection coefficients are used as inputs to further compute the objective function of the optimization problem using (2). The new set of decision variables is updated using (11), (12) and the best social condition is reserved using (13). When the iterative process is completed, the feasible solution of the given optimization problem is obtained.

To obtain a feasible solution from the optimization process described in Fig. 4, the definition of the CO algorithm's parameters is also required. For the given optimization problem of a patch antenna for RF EH applications, we apply the following parameters:

- Total population of coyotes N : 30
- Number of coyote packs N_p : 5
- Number of coyotes in each pack N_c : 6
- Maximum number of iterations $MaxIt$: 1000
- Number of independent trials: 20

TABLE 3. Feasible solution (social condition) of the proposed multiband patch antenna obtained by the optimization process described in Fig. 4.

Variable	Value (mm)	Variable	Value (mm)
L_{patch}	82.63	W_{patch}	44
L_{feeder}	86.40	W_{feeder}	9.09
L_{s1}	4.13	W_{s1}	4.84
L_{s2}	4.96	W_{s2}	8.08
L_{s3}	14.96	W_{s3}	8.26
O_{feeder}	21.48	O_{s1}	8.36
O_{s2}	18.04	O_{s3}	8.26

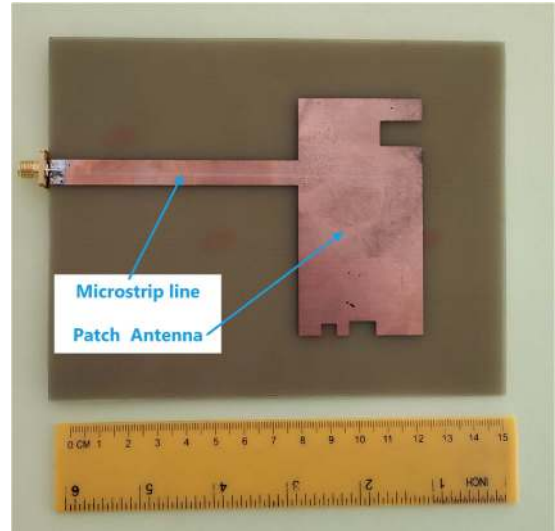


FIGURE 5. Fabricated antenna (the geometry was obtained by the optimization process described in Fig. 4).

V. RESULTS AND DISCUSSION

Table 3 lists the values of the decision variables (social condition) obtained by the optimization process as described in Fig. 4. These values provide a feasible solution to the optimization problem of designing a multiband patch antenna suitable for RF EH applications. Fig. 5 presents the fabricated multiband patch antenna based on the model of Fig. 3(b) and the results of Table 3.

We evaluate the fabricated multiband patch antenna by performing a set of measurements in its main characteristics, i.e., the reflection coefficient (S_{11} magnitude), the radiation pattern in the tuning frequencies, the half-power beamwidth (HPBW), and the gain. For the experimental validation of the proposed antenna, the following equipment was utilized:

- E5062A, ENA-L RF Network Analyzer, 300 kHz to 3 GHz (© 2020 Agilent Technologies, Inc.)
- 8593EM, EMC Analyzer, 9 kHz to 22 GHz (© Keysight Technologies 2000-2020)
- IFR Signal Generator, 9 kHz to 2.51 GHz (© IFR Ltd. 1999)

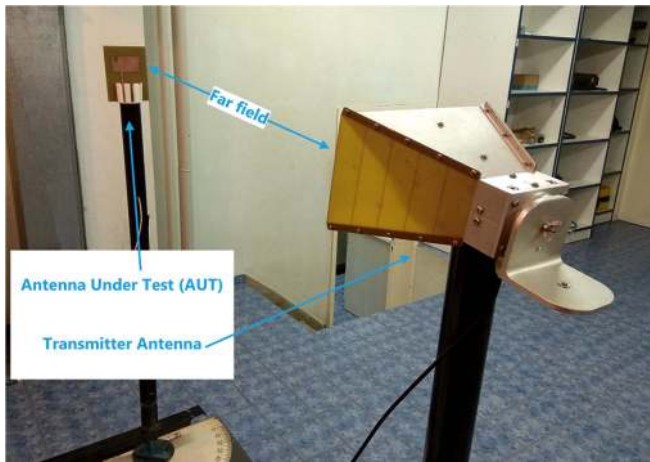


FIGURE 6. Measurement setup (controlled environment).

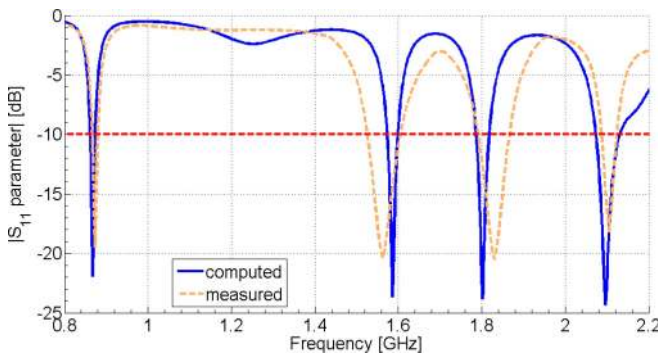


FIGURE 7. S_{11} parameter (reflection coefficient) versus frequency of the multiband patch antenna (blue solid line: computed results, orange dash line: measured results, red dash line: -10 dB limit).

- 3115 Double-Ridged Waveguide Horn Antenna, 750 MHz to 18 GHz (© Keysight Technologies 2000-2020)

Fig. 6 portrays the experimental setup for the performance evaluation of the fabricated multiband patch antenna (Antenna Under Test - AUT) in a controlled environment.

Fig. 7 compares the computed against the measured S_{11} magnitude of the multiband patch antenna versus frequency. From the presented graph it is clear that the proposed antenna has a multi-frequency tuning operation (computed results: -21.94 dB at 867.7 MHz, -23.68 dB at 1585.5 MHz, -23.85 dB at 1801.9 MHz, and -24.33 dB at 2095.8 MHz, measured results: -19.53 dB at 873 MHz, -20.38 dB at 1563 MHz, -20.51 dB at 1830 MHz, and -18.22 dB at 2105 MHz) within the European LoRaWAN frequency band (863 - 870 MHz), as well as the GSM-1800 (1710 - 1880 MHz) and the UMTS (1920.3 - 2155.3 MHz) mobile communication frequency bands. From the measured results we can obtain that the S_{11} bandwidth (-10 dB bandwidth) of the multiband antenna is 15 MHz (865 MHz - 880 MHz), 80 MHz (1525 MHz - 1605 MHz), 78 MHz (1790 MHz - 1868 MHz), and 40 MHz (2085 - 2125 MHz)

TABLE 4. Half Power Beamwidth (HPBW) of the fabricated antenna in the two main planes of interest.

Frequency	XZ plane	YZ plane
867.7 MHz	120 deg	90 deg
1585.5 MHz	100 deg	80 deg
1801.9 MHz	170 deg	93 deg
2095.8 MHz	60 deg	60 deg

TABLE 5. Computed against measured maximum gain values of the proposed multiband patch antenna.

Frequency	Computed gain	Measured gain
867.7 MHz	1.78 dBi	1.29 dBi
1585.5 MHz	3.80 dBi	3.94 dBi
1801.9 MHz	2.18 dBi	1.15 dBi
2095.8 MHz	1.64 dBi	0.89 dBi

at the previously mentioned frequency bands of operation, accordingly.

Fig. 8 compares the computed versus the measured normalized radiation pattern of the multiband patch antenna in the two main planes of interest (XZ plane ($\phi = 0$ deg), YZ plane ($\phi = 90$ deg)). From the depicted graphs we can derive that the proposed patch antenna with three slits exhibits broadside beamwidth at the desired frequency bands in both main planes. Table 4 lists the experimental results of the half-power beamwidth. The maximum HPBW achieved by the fabricated antenna is 170 deg in the frequency band of GSM-1800 and for the XZ plane ($\phi = 0$ deg). From the presented results of Table 4, we can conclude that the proposed patch antenna can be properly performed as an RF energy harvester in the aforementioned frequency bands of operation.

Fig. 9 portrays the realized gain of the multiband patch antenna (feasible solution obtained by the optimization process described in Fig. 4) in a 3D plot and at the frequency bands of interest. Once again, from the presented graphs we can derive that the proposed antenna operates satisfactorily as an RF energy harvesting module in a rectenna system. Table 5 lists the maximum computed and measured gain values of the multiband patch antenna at the tuning frequencies. The measured gain values of the proposed antenna are obtained by utilizing the signal generator, as well as the EMC analyzer, and applying the Friis transmission equation. The maximum measured gain value of the fabricated antenna achieved in the tuning frequency of 1585 MHz and is equal to 3.94 dBi. The maximum deviation between computed and measured results is about 1 dB. It is also noteworthy to indicate the fabricated antenna exhibits acceptable gain values in the frequency bands of European LoRaWAN, as well as in GSM-1800 and UMTS mobile communication systems.

Table 6 lists the comparative results of this work against selected published works in the literature. From the presented results we can find that our proposed antenna exhibits

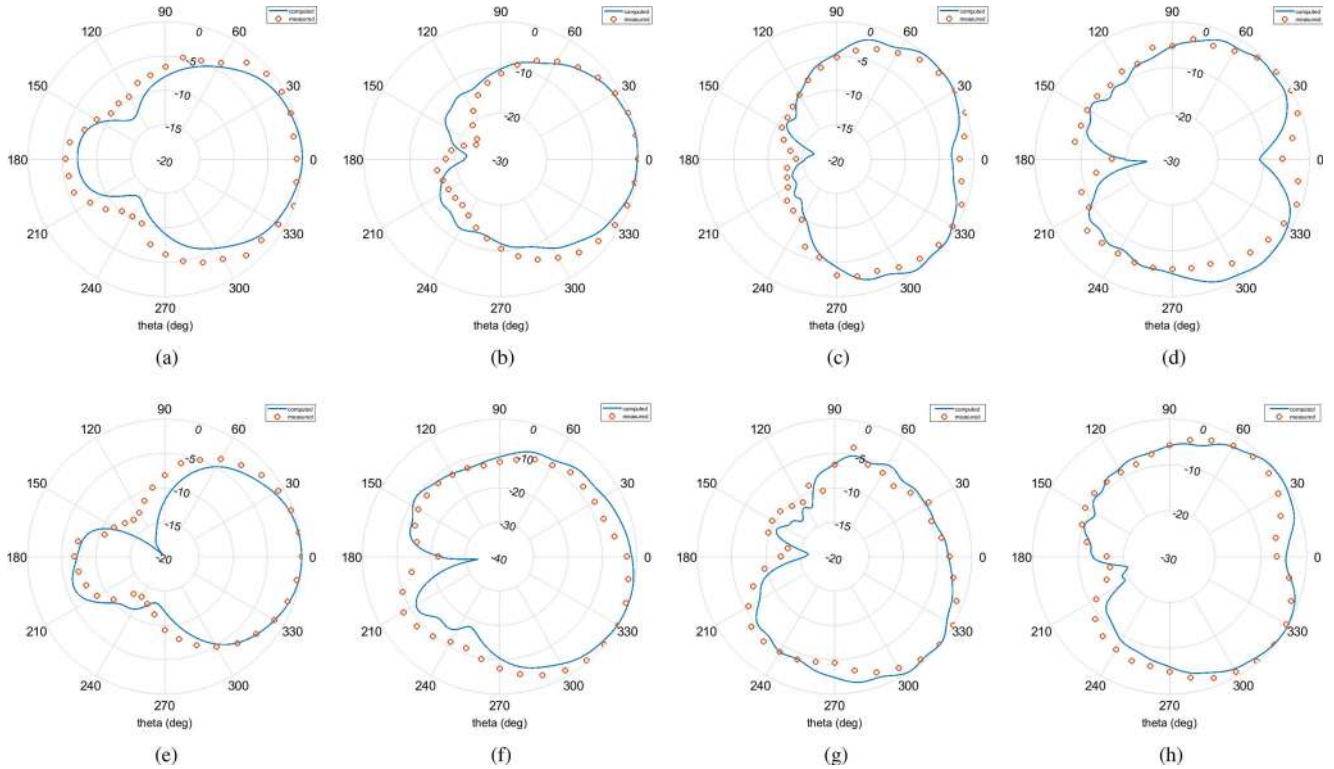


FIGURE 8. Normalized radiation pattern of the multiband patch antenna in two main planes (XZ plane, YZ plane) of interest (blue solid line: computed results, orange circular markers: measured results) (a) freq = 867.7 MHz, $\phi = 0$ deg, (b) freq = 1585.5 MHz, $\phi = 0$ deg, (c) freq = 1801.9 MHz, $\phi = 0$ deg, (d) freq = 2095.8 MHz, $\phi = 0$ deg, (e) freq = 867.7 MHz, $\phi = 90$ deg, (f) freq = 1585.5 MHz, $\phi = 90$ deg, (g) freq = 1801.9 MHz, $\phi = 90$ deg, (h) freq = 2095.8 MHz, $\phi = 90$ deg.

TABLE 6. Comparative results of the proposed multiband patch antenna against related work.

Ref.	Size in λ_0^*	Frequency Bands	Max. Gain
This work	0.24×0.13	LoRa, 1.585 GHz, GSM-1800, UMTS	3.94 dBi
[32]	0.14×0.12	GSM-900, GSM-1800, UMTS, Wi-Fi	2.3 dBi
[36]	0.3×0.3	GSM-900, GSM-1800, UMTS, Wi-Fi	6.0 dBi
[47]	0.62×0.54	GSM-900, GSM-1800, UMTS	8.15 dBi
[50]	0.14×0.12	GSM-900, Wi-Fi, 3.2 GHz, 3.8 GHz	1.6 dBi
[53]	0.29×0.29	0.79 GHz - 0.96 GHz, 1.71 GHz - 2.69 GHz	6.0 dBi

* λ_0 is the wavelength referring to the lowest tuning frequency of antenna operation.

satisfactory results, having an acceptable physical size compared to the wavelength of the lowest operating frequency, operating in four different frequency bands including the European LoRaWAN band, and achieving acceptable gain values. Therefore, from both simulated and measured results, we can conclude that the proposed antenna has features of operation which make it a possible candidate for RF energy

harvesting applications. The multiband patch antenna can be utilized in various wireless-based applications by harvesting energy from the RF environment in order to self-power sensor systems. These applications can include (a) LoRaWAN IoT networks for agricultural or aquacultural sectors, by harvesting RF energy mostly from dedicated sources, (b) LoRaWAN IoT networks for parking seats in a smart city ecosystem, by harvesting RF energy either from dedicated or ambient sources, and (c) mobile communication networks for environmental monitoring, by harvesting RF energy mostly from ambient sources.

VI. CONCLUSION

In this work, we have presented a multiband microstrip patch antenna which is a promising candidate for RF energy harvesting applications. The proposed antenna operates satisfactorily in the European LoRaWAN frequency band, as well as in the GSM-1800 and UMTS mobile communication networks frequency bands. The multiband operation is achieved by introducing three slits of various sizes in the original rectangular patch. The feasible solution of the proposed antenna is obtained by applying an optimization method that combines the Coyote Optimization algorithm and a powerful high-frequency electromagnetic solver. The designed antenna is fabricated and evaluated in a controlled environment. Experimental results of the proposed antenna exhibit acceptable values of key performance markers (size

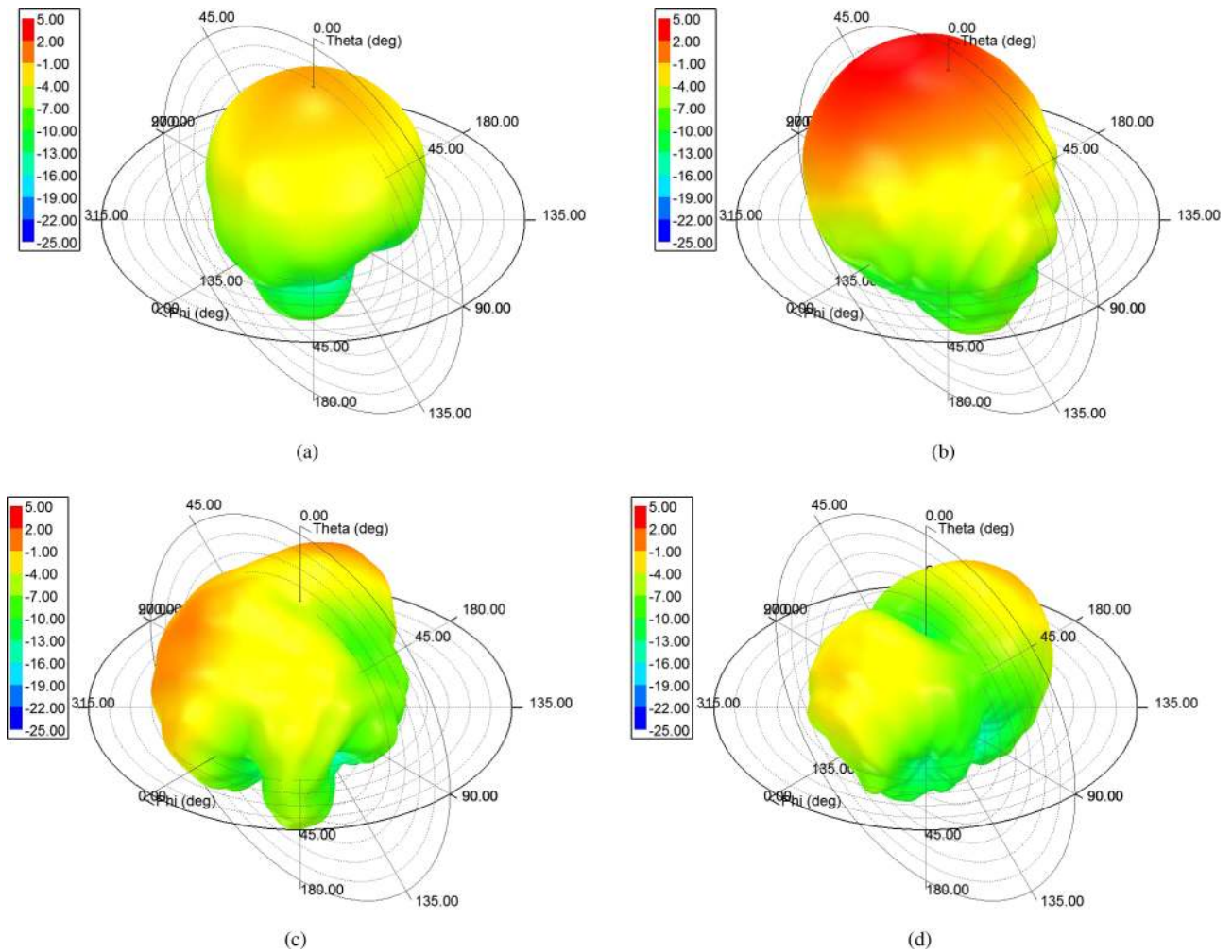


FIGURE 9. Realized gain (gain values including any mismatch) of the multiband patch antenna (feasible solution obtained by the optimization process described in Fig. 4) (color scale in dB) (a) freq = 867.7 MHz, (b) freq = 1585.5 MHz, (c) freq = 1801.9 MHz, and (d) freq = 2095.8 MHz.

of $0.24\lambda_0 \times 0.13\lambda_0$ compared to the wavelength of the lowest frequency of antenna operation, multiband tuning operation including the frequency bands of LoRaWAN, GSM-1800, and UMTS, broadside beamwidth (maximum HPBW of 170 deg), adequate gain (maximum gain of 3.94 dBi), which make it a suitable candidate for RF energy harvesting systems. Future work includes the design and fabrication of the rectifying module, the study of alternative techniques for the antenna feeding, the conduct of harvesting measurements and DC voltage upconversion, and the experimental evaluation of the overall rectenna system.

REFERENCES

- [1] A. Harb, "Energy harvesting: State-of-the-art," *Renew. Energy*, vol. 36, no. 10, pp. 2641–2654, 2011.
- [2] S. Ulukus *et al.*, "Energy harvesting wireless communications: A review of recent advances," *IEEE J. Sel. Areas Commun.*, vol. 33, no. 3, pp. 360–381, Mar. 2015.
- [3] F. K. Shaikh and S. Zeadally, "Energy harvesting in wireless sensor networks: A comprehensive review," *Renew. Sustain. Energy Rev.*, vol. 55, pp. 1041–1054, Mar. 2016.
- [4] M. Wagih, A. S. Weddell, and S. Beeby, "Millimeter-wave power harvesting: A review," *IEEE Open J. Antennas Propag.*, vol. 1, pp. 560–578, 2020.
- [5] X. Lu, P. Wang, D. Niyato, D. I. Kim, and Z. Han, "Wireless networks with RF energy harvesting: A contemporary survey," *IEEE Commun. Surveys Tuts.*, vol. 17, no. 2, pp. 757–789, 2nd Quart., 2015.
- [6] M. Prauzek, J. Konecny, M. Borova, K. Janosova, J. Hlavica, and P. Musilek, "Energy harvesting sources, storage devices and system topologies for environmental wireless sensor networks: A review," *Sensors*, vol. 18, no. 8, p. 2446, 2018.
- [7] S. Kim *et al.*, "Ambient RF energy-harvesting technologies for self-sustainable standalone wireless sensor platforms," *Proc. IEEE*, vol. 102, no. 11, pp. 1649–1666, 2014.
- [8] C. Yuen, M. Elkashlan, Y. Qian, T. Q. Duong, L. Shu, and F. Schmidt, "Energy harvesting communications: Part 1 [guest editorial]," *IEEE Commun. Mag.*, vol. 53, no. 4, pp. 68–69, Apr. 2015.
- [9] J. C. Kwan and A. O. Fapojuwo, "Radio frequency energy harvesting and data rate optimization in wireless information and power transfer sensor networks," *IEEE Sensors J.*, vol. 17, no. 15, pp. 4862–4874, Aug. 2017.
- [10] S. Hemour and K. Wu, "Radio-frequency rectifier for electromagnetic energy harvesting: Development path and future outlook," *Proc. IEEE*, vol. 102, no. 11, pp. 1667–1691, Nov. 2014.
- [11] M. Arrawatia, M. S. Baghini, and G. Kumar, "Differential microstrip antenna for RF energy harvesting," *IEEE Trans. Antennas Propag.*, vol. 63, no. 4, pp. 1581–1588, Apr. 2015.

- [12] A. Georgiadis, G. V. Andia, and A. Collado, "Rectenna design and optimization using reciprocity theory and harmonic balance analysis for electromagnetic (EM) energy harvesting," *IEEE Antennas Wireless Propag. Lett.*, vol. 9, pp. 444–446, 2010.
- [13] A. D. Boursianis *et al.*, "Smart irrigation system for precision agriculture—The Arethou5A IoT platform," *IEEE Sensors J.*, early access, doi: [10.1109/JSEN.2020.3033526](https://doi.org/10.1109/JSEN.2020.3033526).
- [14] A. D. Boursianis, M. S. Papadopoulou, S. Nikolaidis, and S. K. Goudos, "Dual-band single-layered modified e-shaped patch antenna for RF energy harvesting systems," in *Proc. Eur. Conf. Circuit Theory Design (ECCTD)*, 2020, pp. 1–4.
- [15] M. Wagih, A. S. Weddell, and S. Beeby, "Rectennas for radio-frequency energy harvesting and wireless power transfer: A review of antenna design [antenna applications corner]," *IEEE Antennas Propag. Mag.*, vol. 62, no. 5, pp. 95–107, Oct. 2020.
- [16] M. Cansiz, D. Altinel, and G. K. Kurt, "Efficiency in RF energy harvesting systems: A comprehensive review," *Energy*, vol. 174, pp. 292–309, May 2019.
- [17] M. Abdel-Basset, L. Abdel-Fatah, and A. K. Sangaiah, "Chapter 10—Metaheuristic algorithms: A comprehensive review," in *Computational Intelligence for Multimedia Big Data on the Cloud with Engineering Applications* (Intelligent Data-Centric Systems), A. K. Sangaiah, M. Sheng, and Z. Zhang, Eds. New York, NY, USA: Academic, 2018, pp. 185–231.
- [18] X.-S. Yang, *Nature-Inspired Metaheuristic Algorithms*. London, U.K.: Luniver, 2010.
- [19] S. J. Nanda and G. Panda, "A survey on nature inspired metaheuristic algorithms for partitional clustering," *Swarm Evol. Comput.*, vol. 16, pp. 1–18, Jun. 2014.
- [20] S. H. S. Moosavi and V. K. Bardsiri, "Poor and rich optimization algorithm: A new human-based and multi populations algorithm," *Eng. Appl. Artif. Intell.*, vol. 86, pp. 165–181, Nov. 2019.
- [21] P. Rocca, M. Benedetti, M. Donelli, D. Franceschini, and A. Massa, "Evolutionary optimization as applied to inverse scattering problems," *Inverse Problems*, vol. 25, no. 12, Nov. 2009, Art. no. 123003.
- [22] S. Mirjalili, S. M. Mirjalili, and A. Lewis, "Grey wolf optimizer," in *Proc. Adv. Eng. Softw.*, vol. 69, 2014, pp. 46–61.
- [23] S. Mirjalili, A. H. Gandomi, S. Z. Mirjalili, S. Saremi, H. Faris, and S. M. Mirjalili, "SALP swarm algorithm: A bio-inspired optimizer for engineering design problems," *Adv. Eng. Softw.*, vol. 114, pp. 163–191, Dec. 2017.
- [24] S. Mirjalili and A. Lewis, "The whale optimization algorithm," *Adv. Eng. Softw.*, vol. 95, pp. 51–67, May 2016.
- [25] F. J. Villegas, T. Cwik, Y. Rahmat-Samii, and M. Manteghi, "A parallel electromagnetic genetic-algorithm optimization (EGO) application for patch antenna design," *IEEE Trans. Antennas Propag.*, vol. 52, no. 9, pp. 2424–2435, Sep. 2004.
- [26] J. Kennedy and R. Eberhart, "Particle swarm optimization," in *Proc. Int. Conf. Neural Netw. (ICNN)*, vol. 4, 1995, pp. 1942–1948.
- [27] J. Robinson and Y. Rahmat-Samii, "Particle swarm optimization in electromagnetics," *IEEE Trans. Antennas Propag.*, vol. 52, no. 2, pp. 397–407, Feb. 2004.
- [28] D. Simon, "Biogeography-based optimization," *IEEE Trans. Evol. Comput.*, vol. 12, no. 6, pp. 702–713, Dec. 2008.
- [29] S. Kirkpatrick, C. D. Gelatt, and M. P. Vecchi, "Optimization by simulated annealing," *Science*, vol. 220, no. 4598, pp. 671–680, 1983.
- [30] R. V. Rao, V. J. Savsani, and D. Vakharia, "Teaching–learning-based optimization: A novel method for constrained mechanical design optimization problems," *Comput.-Aided Design*, vol. 43, no. 3, pp. 303–315, 2011.
- [31] J. Pierezan, G. Maidl, E. M. Yamao, L. D. S. Coelho, and V. C. Mariani, "Cultural coyote optimization algorithm applied to a heavy duty gas turbine operation," *Energy Convers. Manag.*, vol. 199, Nov. 2019, Art. no. 111932.
- [32] S. Agrawal, M. S. Parihar, and P. N. Kondekar, "A quad-band antenna for multi-band radio frequency energy harvesting circuit," *Int. J. Electron. Commun.*, vol. 85, pp. 99–107, Feb. 2018.
- [33] M. F. Shaker, H. A. Ghali, D. M. N. Elsheakh, and H. A. E. Elsadek, "Multiband coplanar monopole antenna for energy harvesting," in *Proc. IEEE Int. Symp. Radio Freq. Integr. Technol. (RFIT)*, 2018, pp. 1–3.
- [34] N. A. Eltresy, D. M. Elsheakh, and E. A. Abdallah, "Multi-bandwidth CPW-FED open end square loop monopole antenna for energy harvesting," in *Proc. Int. Appl. Comput. Electromagn. Soc. Symp. (ACES)*, 2018, pp. 1–2.
- [35] O. M. A. Dardeer, H. Elsadek, and E. A. Abdallah, "CPW-FED multi-band antenna for various wireless communications applications," in *Proc. IEEE Int. Symp. Antennas Propag. USNC/URSI Nat. Radio Sci. Meeting*, 2018, pp. 785–786.
- [36] V. Kuhn, C. Lahuec, F. Seguin, and C. Person, "A multi-band stacked RF energy harvester with RF-to-DC efficiency up to 84%," *IEEE Trans. Microwaves Theory Techn.*, vol. 63, no. 5, pp. 1768–1778, May 2015.
- [37] A. Nimo, D. Grgić, and L. M. Reindl, "Ambient electromagnetic wireless energy harvesting using multiband planar antenna," in *Proc. Int. Multi Conf. Syst. Signals Devices*, 2012, pp. 1–6.
- [38] M. Picuela, P. D. Mitcheson, and S. Lucyszyn, "Ambient RF energy harvesting in urban and semi-urban environments," *IEEE Trans. Microwaves Theory Techn.*, vol. 61, no. 7, pp. 2715–2726, Jul. 2013.
- [39] B. Singh, S. Ghosh, and S. Chakrabarti, "Design optimization and implementation of multiband rectenna for efficient radio frequency energy harvesting," in *Proc. IEEE Int. Conf. Ind. Inf. Syst. (ICIS)*, 2017, pp. 1–6.
- [40] N. Nguyen *et al.*, "Multiband antenna for RF energy harvesting," in *Proc. Int. Symp. Antennas Propag. (ISAP)*, 2018, pp. 1–2.
- [41] H. S. Khalilq, M. Awais, W. Ahmad, and W. T. Khan, "A high gain six band frequency independent dual CP planar log periodic antenna for ambient RF energy harvesting," in *Proc. Progr. Electromagn. Res. Symp. Fall (PIERS-FALL)*, 2017, pp. 3024–3028.
- [42] S. Keyrouz, H. J. Visser, and A. G. Tjhuis, "Multi-band simultaneous radio frequency energy harvesting," in *Proc. 7th Eur. Conf. Antennas Propag. (EuCAP)*, 2013, pp. 3058–3061.
- [43] N. Singh, B. K. Kanaujia, M. T. Beg, Mainuddin, T. Khan, and S. Kumar, "A dual polarized multiband rectenna for RF energy harvesting," *Int. J. Electron. Commun.*, vol. 93, pp. 123–131, Sep. 2018.
- [44] S. Chandravanshi, S. S. Sarma, and M. J. Akhtar, "Design of triple band differential rectenna for RF energy harvesting," *IEEE Trans. Antennas Propag.*, vol. 66, no. 6, pp. 2716–2726, Jun. 2018.
- [45] S. Shen, Y. Zhang, C. Chiu, and R. Murch, "An ambient RF energy harvesting system where the number of antenna ports is dependent on frequency," *IEEE Trans. Microwaves Theory Techn.*, vol. 67, no. 9, pp. 3821–3832, Sep. 2019.
- [46] K. Gangwar and J. Tissier, "Modified log periodic spiral antenna for multi-band RF energy harvesting applications," in *Proc. IEEE Wireless Power Transfer Conf. (WPTC)*, 2019, pp. 573–577.
- [47] S. Shen, C. Chiu, and R. D. Murch, "A dual-port triple-band L-PROBE microstrip patch rectenna for ambient RF energy harvesting," *IEEE Antennas Wireless Propag. Lett.*, vol. 16, pp. 3071–3074, 2017.
- [48] A. Arora, S. Singh, Vandana, M. Varshney, M. K. Pandey, and S. Pandey, "A novel lotus shaped multiband patch antenna with improved performance," in *Proc. Photon. Electromagn. Res. Symp. Spring (PIERS-Spring)*, 2019, pp. 3571–3577.
- [49] A. G. Koutinos *et al.*, "Modified easy to fabricate e-Shaped compact patch antenna with wideband and multiband functionality," *IET Microwaves Antennas Propag.*, vol. 12, no. 3, pp. 326–331, 2018.
- [50] M. Taghadosi, L. Albasha, N. Qaddoumi, and M. Ali, "Miniaturised printed elliptical nested fractal multiband antenna for energy harvesting applications," *IET Microwaves Antennas Propag.*, vol. 9, no. 10, pp. 1045–1053, 2015.
- [51] A. Bakytbekov, T. Q. Nguyen, C. Huynh, K. N. Salama, and A. Shamim, "Fully printed 3D cube-shaped multiband fractal rectenna for ambient RF energy harvesting," *Nano Energy*, vol. 53, pp. 587–595, Nov. 2018.
- [52] A. B. Jagadeesan, A. Alphones, M. F. Karim, and L. C. Ong, "Metamaterial based reconfigurable multiband antenna," in *Proc. IEEE Int. Symp. Antennas Propag. USNC/URSI Nat. Radio Sci. Meeting*, 2015, pp. 2389–2390.
- [53] V. Palazzi *et al.*, "A novel ultra-lightweight multiband rectenna on paper for RF energy harvesting in the next generation LTE bands," *IEEE Trans. Microw. Theory Techn.*, vol. 66, no. 1, pp. 366–379, Jan. 2018.
- [54] D. Masotti, A. Costanzo, M. Del Prete, and V. Rizzoli, "Genetic-based design of a tetra-band high-efficiency radio-frequency energy harvesting system," *IET Microwaves Antennas Propag.*, vol. 7, no. 15, pp. 1254–1263, 2013.

- [55] R. Pandey, A. K. Shankhwar, and A. Singh, "Design, analysis, and optimization of dual side printed multiband antenna for RF energy harvesting applications," *Progr. Electromagn. Res.*, vol. 102, pp. 79–91, 2020.
- [56] N. Singh *et al.*, "Low profile multiband rectenna for efficient energy harvesting at microwave frequencies," *Int. J. Electron.*, vol. 106, no. 12, pp. 2057–2071, 2019.
- [57] C. Song *et al.*, "A novel six-band dual CP rectenna using improved impedance matching technique for ambient RF energy harvesting," *IEEE Trans. Antennas Propag.*, vol. 64, no. 7, pp. 3160–3171, Jul. 2016.
- [58] J. M. Barcak and H. P. Partal, "Efficient rf energy harvesting by using multiband microstrip antenna arrays with multistage rectifiers," in *Proc. IEEE Subthreshold Microelectron. Conf. (SubVT)*, 2012, pp. 1–3.
- [59] A. Okba, A. Takacs, H. Aubert, S. Charlot, and P.-F. Calmon, "Multiband rectenna for microwave applications," *Comptes Rendus Physique*, vol. 18, no. 2, pp. 107–117, 2017.
- [60] C. Song, P. Lu, and S. Shen, "Highly efficient omnidirectional integrated multi-band wireless energy harvesters for compact sensor nodes of Internet-of-Things," *IEEE Trans. Ind. Electron.*, early access, Jul. 21, 2020, doi: [10.1109/TIE.2020.3009586](https://doi.org/10.1109/TIE.2020.3009586).
- [61] X.-S. Yang, "Firefly algorithm, stochastic test functions and design optimisation," *Int. J. Bio Inspired Comput.*, vol. 2, no. 2, pp. 78–84, 2010.
- [62] D. T. Pham, A. Ghanbarzadeh, E. Koç, S. Otri, S. Rahim, and M. Zaidi, "The bees algorithm—A novel tool for complex optimisation problems," in *Intelligent Production Machines and Systems*. Amsterdam, The Netherlands: Elsevier, 2006, pp. 454–459.
- [63] Z. W. Geem, J. H. Kim, and G. V. Loganathan, "A new heuristic optimization algorithm: Harmony search," *Simulation*, vol. 76, no. 2, pp. 60–68, 2001.
- [64] M. Dorigo, M. Birattari, and T. Stutzle, "Ant colony optimization," *IEEE Comput. Intell. Mag.*, vol. 1, no. 4, pp. 28–39, Nov. 2006.
- [65] S. Surjanovic and D. Bingham. (Dec. 21, 2020). *Virtual Library of Simulation Experiments: Test Functions and Datasets*. [Online]. Available: <http://www.sfu.ca/ssurjano>

ACHILLES D. BOURSISIANIS (Member, IEEE) received the B.Sc. degree in physics, the M.Sc. degree in electronic physics (radioelectrology) in the area of electronics telecommunications technology, and the Ph.D. degree in telecommunications from the School of Physics, Aristotle University of Thessaloniki in 2001, 2005, and 2017, respectively.

Since 2019, he has been serving as a Postdoctoral Researcher and an Academic Fellow with the School of Physics, Aristotle University of Thessaloniki. He is also a member of the ELEDIA@AUTH Research Group. He has authored or coauthored more than 40 articles in international peer-reviewed journals and conferences. His research interests include wireless sensor networks, Internet of Things, antenna design and optimization, 5G communication networks, radio frequency energy harvesting, and artificial intelligence.

Dr. Boursisianis serves as a reviewer of several international journals and conferences and as a member of the technical program committees of various international conferences, which were technically sponsored by IEEE. He is a member of the Editorial Board of *Telecom*. He is a member of the Hellenic Physical Society and the Scientific Committee of the National Association of Fédération des Ingénieurs des Télécommunications de la Communauté Européenne.

MARIA S. PAPAPOPOULOU received the Ph.D. degree from the School of Physics, Aristotle University of Thessaloniki (AUTH). Since 2014, she has been serving as a Visiting Lecturer with the Department of Information and Electronic Engineering, International Hellenic University. She is a Senior Researcher with the School of Physics, AUTH, and she holds a Postdoctoral Research Scholarship. She is also a member of the ELEDIA@AUTH Research Group. She has authored or coauthored several peer-reviewed journals and conferences. Her research interests include nonlinear dynamics, chaotic cryptography, RF energy harvesting, wireless sensor networks, Internet of Things, and electronic design and optimization. She is a member of the Hellenic Physical Society.

JULIANO PIEREZAN received the B.S. degree in electrical engineering from the Pontifical Catholic University of Paraná (PUCPR), Brazil, in 2014, the M.S. and Doctoral degrees in electrical engineering from the Federal University of Paraná (UFPR), Brazil, in 2016 and 2020, respectively. His research interests include optimization, computational intelligence, and machine learning.

VIVIANA C. MARIANI received the Ph.D. degree from the Federal University of Santa Catarina, Brazil. Since 2002, she has been an Associate Professor with the Department of Mechanical Engineering, Pontifical Catholic University of Paraná (PUCPR), Brazil, and an Associate Professor with the Department of Electrical Engineering, Federal University of Paraná (UFPR), Brazil. She has authored or coauthored several peer-reviewed journals and conferences. Her research interests include optimization techniques, machine learning, thermal science, fluid mechanic, and heat exchanger devices.

LEANDRO S. COELHO received the first B.S. degree in computer science and the second B.S. degree in electrical engineering from the Federal University of Santa Maria, Brazil, in 1994 and 1999, respectively, and the M.S. degree in computer science and the Doctoral degree in electrical engineering from the Federal University of Santa Catarina, Brazil, in 1997 and 2000, respectively. He was a Postdoctoral Researcher with the Università degli Studi di Padova, Padua, Italy, in 2019. He is an Associate Professor with the Pontifical Catholic University of Paraná (PUCPR), Brazil, and an Associate Professor with the Electrical Engineering Department, UFSC, Brazil. His research interests include nonlinear artificial intelligence, data science, machine learning, deep learning, and metaheuristics.

PANAGIOTIS SARIGIANNIDIS (Member, IEEE) received the B.Sc. and Ph.D. degrees in computer science from the Aristotle University of Thessaloniki, Thessaloniki, Greece, in 2001 and 2007, respectively.

He has been an Associate Professor with the Department of Electrical and Computer Engineering, University of Western Macedonia, Kozani, Greece, since 2016. He has been involved in several national, European, and international projects. He is currently the Project Coordinator of three H2020 projects, namely: 1) H2020-DS-SC7-2017 (DS-07-2017), SPEAR: Secure and PrivatE smArt gRid; 2) H2020-LC-SC3-EE-2020-1 (LC-SC3-EC-4-2020), EVIDENT: bEhaVioral Insights and Effective eNergy policy aCTions; and 3) H2020-ICT-2020-1 (ICT-56-2020), TERMINET: nexT gEneRation sMart INterconnectEd IoT, while he coordinates the Operational Program MARS: sMart fArming with dRoneS (Competitiveness, Entrepreneurship, and Innovation). He also serves as a Principal Investigator with the H2020-SU-DS-2018 (SU-DS04-2018), SDN-microSENSE: SDN-microgrid reSilient Electrical eNergy SystEm, and in the Erasmus+ KA2 ARRANGE-ICT: pArtnErship foR AddressiNG mEgatrends in ICT (Cooperation for Innovation and the Exchange of Good Practices). He has published over 170 papers in international journals, conferences, and book chapters, including *IEEE COMMUNICATIONS SURVEYS AND TUTORIALS*, *IEEE INTERNET OF THINGS*, *IEEE TRANSACTIONS ON BROADCASTING*, *IEEE SYSTEMS JOURNAL*, *IEEE Wireless Communications Magazine*, *IEEE/OSA JOURNAL OF LIGHTWAVE TECHNOLOGY*, *IEEE ACCESS*, and *Computer Networks*. His research interests include telecommunication networks, Internet of Things, and network security.

Dr. Coelho has participated in the Editorial Boards of various journals, including *International Journal of Communication Systems* and *EURASIP Journal on Wireless Communications and Networking*.

STAVROS KOULOURIDIS (Member, IEEE) was born in Athens, Greece, in 1975. He received the Diploma Engineering degree in electrical and computer engineering and the Ph.D. degree in microwave engineering from the National Technical University of Athens, Greece, in 1999 and 2003, respectively.

From 1999 to 2003, he worked as a Research Engineer with the Microwave and Fiber Optics Lab and Biomedical Simulations and Imaging Unit, National Technical University of Athens. He taught several classes with the School of Pedagogic and Technological Education (ASPAlTE) from 2000 to 2003. From 2000 to 2002, he was also a Teaching Assistant with the National Technical University of Athens. From 2004 to 2008, he worked as a Postdoctoral Researcher with the Electroscience Laboratory, Ohio State University, Columbus, OH, USA. In March 2009, he joined the Electrical and Computer Engineering Department, University of Patras, Greece, and since March 2020, he has been holding an Associate Professor position. From 2015 to 2016, he was visited the Group of Electrical Engineering—Paris (GeePs)/CNRS-CentraleSupélec, University Paris-Sud—Université Paris-Saclay—Sorbonne Université on a Sabbatical leave. He leads the Microwave Communications Group. He has published over 90 refereed journals and conference proceeding papers. His research interests include antenna and microwave devices design, development and fabrication of novel materials, microwave applications in medicine, electromagnetic optimization techniques, and applied computational electromagnetics.

Dr. Koulouridis was the recipient of the Three Year Ph.D. Scholarship on Biomedical Engineering from Hellenic State Scholarships Foundation in 2001. In May 2005, he received the Annual Award for the Best Dissertation in National Technical University of Athens. He was the Chair of IEEE AP/MTT/ED Joint Local Greek Chapter from 2013 to 2019. He was the General Chair of IWAT 2017 (International Workshop in Antennas Technology). He is serving as a reviewer for several scientific international journals. From 2010 to 2019, he served on the Technical Program Committee of IEEE Antennas and Propagation Society International Symposium. Since 2015, he has been serving on the Technical Program Committee of European Conference of Antennas and Propagation as a Meta-Reviewer. He is a Topic Editor of *Electronics* (MDPI) Open Access Journal. He is an Associate Editor of IEEE ANTENNAS AND WIRELESS PROPAGATION LETTERS and IEEE JOURNAL OF ELECTROMAGNETICS, RF AND MICROWAVES IN MEDICINE AND BIOLOGY.

SOTIRIOS K. GOUDOS (Senior Member, IEEE) received the B.Sc. degree in physics, the M.Sc. degree in electronics, and the Ph.D. degree in physics from the Aristotle University of Thessaloniki in 1991, 1994, and 2001, respectively, the master's degree in information systems from the University of Macedonia, Greece, in 2005, and the Diploma degree in electrical and computer engineering from the Aristotle University of Thessaloniki in 2011.

In 2013, he joined the Department of Physics, Aristotle University of Thessaloniki, where he is currently an Associate Professor. He is the Director of the ELEDIA@AUTH Lab member of the ELEDIA Research Center Network. He was the Editor of the book *Microwave Systems and Applications* (In Tech, 2017). His research interests include antenna and microwave structures design, evolutionary algorithms, wireless communications, and semantic Web technologies. He was the Sub-Committee Chair of the Asian–Pacific Microwave Conference 2017 in the track of smart and reconfigurable antennas. He has served as the Technical Program Chair of the International Conference on Modern Circuits and Systems Technologies. He is the Founding Editor-in-Chief of the *Telecom* (MDPI) Open Access Journal. He is currently serving as an Associate Editor for IEEE ACCESS and IEEE OPEN JOURNAL OF THE COMMUNICATION SOCIETY. He was the Lead Guest Editor with the Special Issues of the *International Journal of Antennas and Propagation* with topic Evolutionary Algorithms Applied to Antennas and Propagation: Emerging Trends and Applications in 2016 and 2017. He was also the Lead Guest Editor for the Special Issue of the *EURASIP Journal on Wireless Communications and Networking* in 2018, with a topic Optimization Methods for Key Enabling Technologies: 5G, the IoT, and Big Data. He is also a member of the Editorial Board of the *International Journal of Antennas and Propagation*, the *EURASIP Journal on Wireless Communications and Networking*, and the *International Journal on Advances on Intelligent Systems*. He is also a member of the topic board of the *Electronics* open access journal. He has also served as a member of the technical program committees of several IEEE and non-IEEE conferences. He is a member of IEICE, Greek Physics Society, Technical Chamber of Greece, and the Greek Computer Society.